

Color segmentation by fuzzy co-clustering of chrominance color features

Madasu Hanmandlu ^{a,1}, Om Prakash Verma ^b, Seba Susan ^{a,*}, V.K. Madasu ^c

^a IIT Delhi, New Delhi, India

^b Delhi Technological Univ., Delhi, India

^c Queensland Univ., Brisbane, Australia



ARTICLE INFO

Article history:

Received 19 December 2011

Received in revised form

19 September 2012

Accepted 22 September 2012

Available online 2 April 2013

Keywords:

Fuzzy Co-clustering

Object membership

Feature membership

Validity measure

Bacterial Foraging

Color segmentation

ABSTRACT

This paper presents a novel color segmentation technique using fuzzy co-clustering approach in which both the objects and the features are assigned membership functions. An objective function which includes a multi-dimensional distance function as the dissimilarity measure and entropy as the regularization term is formulated in the proposed fuzzy co-clustering for images (FCCI) algorithm. The chrominance color cues a^* and b^* of CIELAB color space are used as the feature variables for co-clustering. The experiments are conducted on 100 natural images obtained from the Berkeley segmentation database. It is observed from the experimental results that the proposed FCCI yields well formed, valid and high quality clusters, as verified from Liu's F -measure and Normalized Probabilistic RAND index. The proposed color segmentation method is also compared with other segmentation methods namely Mean-Shift, NCUT, GMM, FCM and is found to outperform all the methods. The bacterial foraging global optimization algorithm gives image specific values to the parameters involved in the algorithm.

© 2013 Elsevier B.V. All rights reserved.

1. Introduction

The segmentation of color images is a potential area of research due to its practical significance in various fields. Image segmentation partitions the image into regions/segments such that pixels belonging to a region are more similar to each other than those belonging to different regions. Clustering is a well known approach for segmenting images. It strives to assess the relationships among patterns of the data set by organizing them into groups or clusters such that patterns within a cluster are more similar to each other than those belonging to different clusters. Many algorithms for both hard and fuzzy clustering have been developed to achieve this purpose. In hard clustering, data is divided into crisp clusters, where each data belongs to exactly one cluster. In fuzzy clustering, the data points can belong to more than one cluster, and associated with each of the points are membership grades that indicate the degree to which the data points belong to the different clusters. Clustering in the color domain gives improved segmentation results since color components carry more information than the gray scale components.

Several techniques have been proposed in the field of color segmentation. Histogram based segmentation of color [1] is one of the existing techniques. But it does not guarantee contiguity of the resulting regions. Edge detection based techniques [2] pose the difficulty of determining the boundary of an image due to the ambiguity of the response of a weak edge. Recently, Arbelaez et al. in [3] have proposed a hierarchical segmentation obtained from the output of a contour detector which overcomes the difficulties of weakly linked boundaries. In [4] color segmentation by region growing and merging is investigated. One drawback of the conventional region growing technique is the selection of the seed point and the order in which regions grow or merge. In [5], the problem of seed selection is solved by using the relaxation labeling technique which yields satisfactory results. Recent techniques for region growing use automated seed selection process as in [6] which uses a fuzzy similarity and fuzzy distance based approach. In [7], after the region growing of similar color, Markov Random Fields (MRF) are applied to improve the results. However, it is observed that some homogeneous regions may get disconnected due to the MRF process. Blobworld [8], a popular image segmentation and retrieval algorithm groups pixels into regions by modeling the joint distribution of color texture and position features by a mixture of Gaussians with parameters being decided by the expectation maximization algorithm. However, the resulting blobs may not contain all the details of objects and also may not distinguish an object which is not visually distinct. Further an iterative post-processing step is required to correct the

* Corresponding author. Tel.: +91 98 68850209.

E-mail addresses: mhmanlu@iitd.ac.in (M. Hanmandlu), opverma.dce@gmail.com (O.P. Verma), sebasusan@indiatimes.com, seba_406@yahoo.in (S. Susan), v.madasu@uq.edu.au (V.K. Madasu).

¹ Senior Member IEEE.

mis-alignment of object boundaries. Mean-Shift filtering [9] and Graph partitioning [10,11] methods and their hybrids [12] perform clustering in feature-space and are found to be effective for color segmentation. But they are very sensitive to the parameters like color bandwidth (Mean-Shift) and the threshold edge length (Graph method). Neural network based approaches [13,14] for image segmentation like Competitive Learning Neural Network (CLNN) and Self Organizing of Kohonen Feature Map (SOFM) avoid complex programming but usually consume a lot of training time. Other significant works on image segmentation include: Watershed technique[15] based on the morphological watershed transform, segmentation using the K-nearest neighbor (K-NN) technique [16] which is sensitive to the choice of reference sample and JSEG [17]—a segmentation algorithm based on color and texture. Various combinations of popular segmentation algorithms like region merging and graph partitioning [18], mean-shift and region merging [19], watershed and Kohonen SOM [20] have been suggested together with their advantages. In [21], color segmentation is carried out by applying a set of fuzzy if-then-rules on 200 fixed color samples. The Fuzzy C-Means (FCM) clustering method, a popular choice for color segmentation has been investigated in the works of [22]. The results are quite good but for the computational complexity and sensitivity to the initialization. Several variants of FCM are summarized in [14]. In [23] fuzzy set theory and maximum fuzzy entropy principle are used to convert the image to the fuzzy domain and a Space Scale filter is used to analyze the homogeneity histogram to find the appropriate segments. Fuzzy co-clustering algorithm with its dual fuzzy (object and feature) membership functions was originally derived for document clustering, examples being FCCM, FCoDoK [24,25] and robust versions PFCC [26], RFCC[27]. The co-clustering done so far on images [28,29] is limited to indexing of images for Content based image retrieval (CBIR) in which low level semantic features derived from image histogram are the feature variables for clustering.

In this paper the Fuzzy co-clustering approach is adapted for the segmentation of natural images. An algorithm for the Fuzzy Co-clustering of images (FCCI) is developed by incorporating the distance between each feature data point and the feature cluster center as the dissimilarity measure and the entropies of the objects and features as the regularization terms in the objective function. To prove the effectiveness of our approach we apply the FCCI algorithm for the segmentation of color images with successful results. Some preliminary work on color segmentation of histo-pathological images is reported in [30] and this serves as a precursor to the main work. The CIELAB color space is favored for our experiments due to the wide range of colors possible and its closeness to the human perception system [31], and its chrominance color vector $\{a^*, b^*\}$ is proved to be the best feature combination for the segmentation task [32]. It is found from the experimental results that the color segmentation results obtained by the proposed technique are of high quality with respect to both Liu's evaluation measure and NPR index which are global segmentation evaluation measures and also outperforms over other popular color segmentation methods. The choice of the number of clusters for the experiment is determined in a novel manner by plotting Xie and Beni's cluster validity [33] as the number of clusters is increased and by checking for the first local minima of the curve. The resulting segmentation offers a good tradeoff between color difference and human perception.

The organization of the paper is as follows: The Fuzzy Co-Clustering algorithm for Images (FCCI) is introduced in [Section 2](#). While minimizing the objective function in FCCI, Bacterial Foraging is adapted for global learning of parameters. Later in [Section 3](#), the proposed algorithm is applied for the color segmentation together with the state of the art comparisons. Finally conclusions from over-all results are given in [Section 4](#).

2. Fuzzy co-clustering algorithm for images

2.1. Motivation for the algorithm and related work

Co-clustering simultaneously clusters both objects and features together [24]. This provides two membership functions: the partition or object membership function and the ranking or the feature membership function. The latter serves to filter out the relevant features only during the computation of the object membership function and thus solves the problem of sparseness of data by reducing the dimensionality. The co-clustering algorithm is thus suited to applications with large dimensions and is found to be apt for our experiments on multi-feature color images. The problem of outliers is also minimized by using feature membership function [26]. The problem with using only the feature memberships is that it may lead to coincident/overlapping clusters therefore highlighting the need for both feature and object memberships. Further we include the distance function of feature data points from the feature cluster centroids in the co-clustering process to create richer co-clusters than other fuzzy co-clustering algorithms. The inclusion of the distance factor in the degree of aggregation reduces the optimization problem to a minimization one. In this work co-clustering is integrated with the Fuzzy approach with a view to obtain distinct clusters [24,26]. Both the object and feature memberships in the proposed method are fuzzy, i.e. the object membership is calculated when different clusters compete for a data point and feature memberships are defined when different features compete for a cluster. Thus we have two constraints on the two fuzzy memberships (object and feature memberships) in our method.

Therefore the aim is to have a co-clustering algorithm with the following advantages:

1. It must be insensitive to initialization and form distinct clusters. (Fuzzy clustering)
2. It should perform well in high dimensions and provide well defined clusters. (Co-clustering)
3. It should minimize the impact of outliers to improve the accuracy of co-clustering. (Ranking/Feature memberships)
4. Its objective function should integrate the distance measure of input features w.r.t. feature centroids into the entropy regularization framework.
5. It must be reasonably fast enough.

Several maximum entropy clustering algorithms and their variants are available in the literature [34,35]. One such approach of interest to the present work is the variant of FCM which props on entropy regularization [36]. It involves the minimization of the following objective function:

$$J_{FCM} = \sum_{c=1}^C \sum_{i=1}^N u_{ci} \text{Dist}(x_i, p_c) + T_U \sum_{c=1}^C \sum_{i=1}^N u_{ci} \log u_{ci} \quad (1)$$

subject to the constraint

$$\sum_{c=1}^C u_{ci} = 1, u_{ci} \in [0,1], \forall i = 1, \dots, N \quad (2)$$

where the symbols C, N represent the number of clusters and data points respectively, u_{ci} the fuzzy membership function, T_U the weight factor in the entropy term, $\text{Dist}(x_i, p_c)$ the dissimilarity term equal to the square of the Euclidean distance between pixel x_i and cluster center p_c .

The first term in the R.H.S of (1) denotes the effective squared distance; the second term is the entropy which serves as a regulating factor during the minimization process. The proposed approach aims at co-clustering in the entropy framework of FCM. For this we begin by replacing the distance function $\text{Dist}(x_i, p_c)$ with

$Dist(x_{ij}, p_{cj})$ in the proposed objective function. $Dist(x_{ij}, p_{cj})$ is computed for each feature $j=1,2,\dots,K$ separately.

2.2. Formulating the objective function

Let $X = \{x_1, x_2, \dots, x_i, \dots, x_N\} \in \mathbb{R}^K$ be the set of N data points associated with an image I of size $N_1 \times N_2 = N$, and K is the dimension of the feature space associated with each data point. Let x_{ij} denote the j th feature of the i^{th} data point, $P = \{p_{cj}\}$ be the set of feature cluster centers and $D_{cij} = Dist(x_{ij}, p_{cj})$ be the square of the Euclidean distance between feature data point x_{ij} and the feature cluster centroid p_{cj} given by

$$D_{cij} = d^2(x_{ij}, p_{cj}) = (x_{ij} - p_{cj})^2 \quad (3)$$

Let u_{ci} denotes the object membership of the i th data point to cluster c , $U = \{u_{ci}\}$ be the $C \times N$ object membership function matrix of image I , v_{cj} denotes the feature membership defined as the membership of feature j to the c th cluster and $V = \{v_{cj}\}$ be the corresponding $C \times K$ feature membership matrix for image I .

Including the feature membership function v_{cj} in the first term of (1) and replacing the distance function by $D_{cij} = Dist(x_{ij}, p_{cj})$ yields $\sum_{c=1}^C \sum_{i=1}^N \sum_{j=1}^K u_{ci} v_{cj} D_{cij}$, which is regarded as the degree of aggregation of the proposed objective function J_{FCCI} . Separate entropy regularizing terms $\sum_{c=1}^C \sum_{i=1}^N u_{ci} \log u_{ci}$ and $\sum_{c=1}^C \sum_{j=1}^K v_{cj} \log v_{cj}$ for the object and feature membership functions constitute the second and third terms of J_{FCCI} respectively. Minimizing these two terms is equivalent to maximizing the fuzzy entropies $-\sum_{c=1}^C \sum_{i=1}^N u_{ci} \log u_{ci}$ and $-\sum_{c=1}^C \sum_{j=1}^K v_{cj} \log v_{cj}$. The entropies are maximized when the fuzzy memberships u_{ci} and v_{cj} are uniformly distributed according to their constraints i.e. $u_{ci} = 1/C$ and $v_{cj} = 1/K$.

The objective function J_{FCCI} resulting from combining all the above terms is

$$\begin{aligned} J_{FCCI}(U, V, P) = & \sum_{c=1}^C \sum_{i=1}^N \sum_{j=1}^K u_{ci} v_{cj} D_{cij} + T_U \sum_{c=1}^C \sum_{i=1}^N u_{ci} \log u_{ci} \\ & + T_V \sum_{c=1}^C \sum_{j=1}^K v_{cj} \log v_{cj} \end{aligned} \quad (4)$$

the above expression is minimized subject to the following constraints:

$$\sum_{c=1}^C u_{ci} = 1, u_{ci} \in [0, 1], \forall i = 1, \dots, N \quad (5)$$

$$\sum_{j=1}^K v_{cj} = 1, v_{cj} \in [0, 1], \forall c = 1, \dots, C \quad (6)$$

The minimization of the first term in (4) assigns to the object a higher membership value taking into account the feature cluster center it is closest to and which is more relevant than other features for that particular cluster. The inner product $\{v_{cj} D_{cij}\}$ assigns a higher weight to the distance function pertaining to the prominent features and a lower weight to that of the irrelevant features. The first term therefore denotes the effective squared distance. The second and third entropy regularization terms combine all u_{ci} s and v_{cj} s separately. These contribute to the fuzziness in the resulting clusters. T_U and T_V are the weighting parameters that specify the degree of fuzziness. Increasing T_U and T_V increases the fuzziness of the clusters.

2.3. Deriving the update equations

The constrained optimization problem of FCCI can now be defined from (4) by applying the Lagrange multipliers λ_i and γ_c to

constraints (5) and (6) respectively as shown below.

$$\begin{aligned} J(U, V, P) = & \sum_{c=1}^C \sum_{i=1}^N \sum_{j=1}^K u_{ci} v_{cj} D_{cij} + T_U \sum_{c=1}^C \sum_{i=1}^N u_{ci} \log u_{ci} \\ & + T_V \sum_{c=1}^C \sum_{j=1}^K v_{cj} \log v_{cj} + \sum_{i=1}^N \lambda_i \left(\sum_{c=1}^C u_{ci} - 1 \right) + \sum_{c=1}^C \gamma_c \left(\sum_{j=1}^K v_{cj} - 1 \right) \end{aligned} \quad (7)$$

Taking the partial derivative of $J(U, V, P)$ in (7) with respect to U and setting the gradient to zero we have,

$$\frac{\partial J}{\partial U} = \sum_{j=1}^K v_{cj} D_{cij} + T_U (1 + \log u_{ci}) + \lambda_i = 0 \quad (8)$$

Subjecting u_{ci} derived from (8) to the constraint in (5) the formula for computing the object membership function u_{ci} reduces to,

$$u_{ci} = \frac{e^{-\left(-\sum_{j=1}^K \frac{v_{cj} D_{cij}}{T_U}\right)}}{\sum_{c=1}^C e^{-\left(-\sum_{j=1}^K \frac{v_{cj} D_{cij}}{T_U}\right)}} \quad (9)$$

In a similar manner, taking the partial derivative of $J(U, V, P)$ with respect to V and setting the gradient to zero we have,

$$\frac{\partial J}{\partial V} = \sum_{i=1}^N u_{ci} D_{cij} + T_V (1 + \log v_{cj}) + \gamma_c = 0 \quad (10)$$

Applying the constraint (6) to v_{cj} derived from (10), we obtain the formula for the feature membership function v_{cj} as

$$v_{cj} = \frac{e^{-\left(-\sum_{i=1}^N \frac{u_{ci} D_{cij}}{T_V}\right)}}{\sum_{j=1}^K e^{-\left(-\sum_{i=1}^N \frac{u_{ci} D_{cij}}{T_V}\right)}} \quad (11)$$

Taking the partial derivative of $J(U, V, P)$ with respect to P and setting the gradient to zero we have

$$\frac{\partial J}{\partial P} = v_{cj} \sum_{i=1}^N u_{ci} x_{ij} - v_{cj} p_{cj} \sum_{i=1}^N u_{ci} = 0 \quad (12)$$

Solving (12) yields the formula for p_{cj} as

$$p_{cj} = \frac{\sum_{i=1}^N u_{ci} x_{ij}}{\sum_{i=1}^N u_{ci}} \quad (13)$$

The solution of the constrained optimization problem in (7) can be approximated by Picard iteration or Alternating Optimization (AO) [37] through (9), (11) and (13) which are the update equations for the object, feature memberships and the cluster centroids respectively in each iteration. Optimal partitions U^* of X can be obtained by solving for (U^*, V^*, P^*) at the local minima of J_{FCCI} . The proof of convergence of the FCCI algorithm to a local optimum is given in Appendix A. Since U^*, V^* and P^* are unknowns, the objective function in (4) is neither concave nor convex and usually has many local optima. To find a global optimum of the constrained optimization problem, the FCCI algorithm is further given as a learning step to the Bacterial Foraging algorithm which optimizes the values of the weight parameters T_U and T_V .

2.4. Pseudo-code of FCCI algorithm

1. Initialize the parameters T_U , T_V , maximum error limit ϵ and maximum number of iterations τ_{\max} .
2. Set iteration number $\tau = 1$.
3. Initialize u_{ci} such that $0 \leq u_{ci} \leq 1$.
4. REPEAT

5. Calculate p_{cj} using (13).
6. Calculate D_{cij} using (3).
7. Calculate v_{cj} using (11).
8. Calculate u_{ci} using (9).
9. Calculate $\tau = \tau + 1$.
10. UNTIL $\max(|u_{ci}(\tau) - u_{ci}(\tau-1)|) \leq \epsilon$ or $\tau = \tau_{max}$.

Since all our experiments are found to converge within 200 iterations, $\tau_{max}=200$ and the maximum error limit ϵ taken to be 10^{-2} .

3. Color image segmentation using FCCI

3.1. A. Algorithm for color segmentation

3.1.1. Review of Xie and Beni's cluster validity S

According to Xie and Beni [33] the validity function S of the clusters for the worst case is defined by

$$S = \frac{\sigma/N}{d_{min}^2} \quad (14)$$

The d_{min} in (14) is evaluated from

$$d_{min} = \min_{\forall c} \left\{ \sum_{j=1}^K (p_{(c+1)j} - p_{cj})^2 \right\} \quad (15)$$

where d_{min} is the minimum distance between the cluster centroids p_{cj} for cluster $c=1, \dots, C$ and feature j and σ is the maximum variation among all the clusters C , given by

$$\sigma = \max_{\forall c} \left\{ \sum_{i=1}^N u_{ci}^2 \sum_{j=1}^K (x_{ij} - p_{cj})^2 \right\} \quad (16)$$

To determine the number of clusters based on the above Cluster Validity S a flowchart is given in Fig. 1 which checks for the occurrence of the first local minima of S .

3.2. Algorithm for color image segmentation using FCCI

The algorithm is outlined as follows:

1. Obtain the three dimensional RGB input image.
2. Convert RGB color space into the CIELAB color space with color dimensions $K=2$, i.e. $\{a^*, b^*\}$.
3. Perform 2D to 1D transformation [38] (by lifting the elements columnwise) to generate data point x_{ij} in the j th dimension, $j=1, 2$ for each pixel $i=1, \dots, N$, where N is the size of the data. This step is important since the computations become simpler when data is one dimensional rather than two dimensional.
4. Determine the number of clusters C as per the flowchart in Fig. 1.
5. Run the FCCI algorithm for C clusters and obtain the object u_{ci} membership function.
6. Defuzzify u_{ci} into clusters.

3.3. B. Bacterial Foraging for the global minimum

The Bacterial Foraging (BF) [39] based on the bacterial chemotactic behavior of *E. Coli* is used for optimizing the values of fuzzy parameters T_U and T_V in the FCCI algorithm. The BF algorithm initially accepts a set of initial values from the user before optimizing these to global minimum values by subsequent iterations. The following initial values: $T_U = 10$, $T_V = 9 \times 10^7$ are assumed for the color segmentation experiments. The choice of these initial values is made by conducting a set of random experiments by hit and trial. Bacterial Foraging is treated as an optimization process

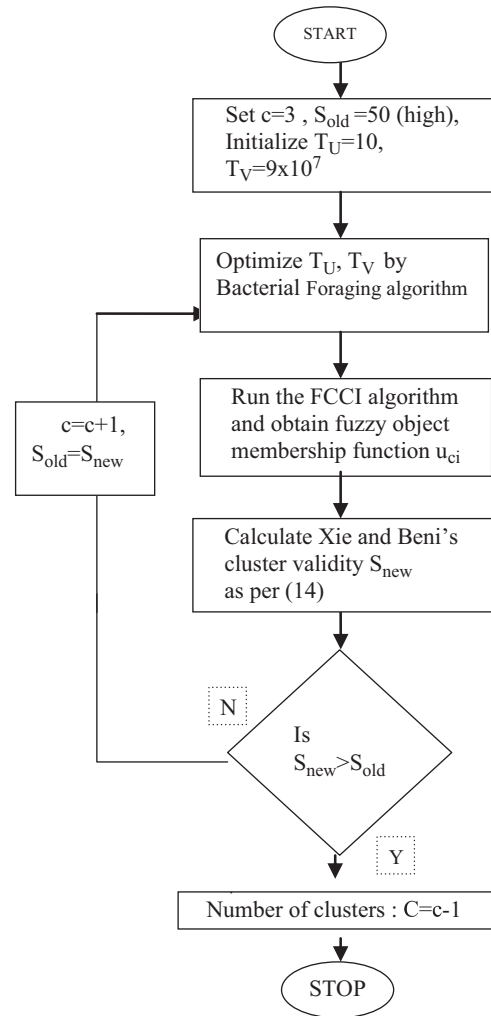


Fig. 1. Flowchart for determining the number of clusters.

[40], where each bacterium seeks to maximize the energy obtained per unit time spent on foraging. Suppose that θ is the position of a bacterium and let $J_D(\theta)$ represent the combined effects of attractants and repellents from the environment, for e.g. $J_D(\theta) < 0$, $J_D(\theta)=0$, $J_D(\theta) > 0$, representing that the bacterium at location is in nutrient rich, neutral, and noxious environments, respectively.

Chemotaxis is a foraging behavior that implements a type of optimization where bacteria try to climb up the nutrient concentration (i.e. find lower and lower values of $J_D(\theta) < 0$ termed as swim), avoid noxious substances (for $J_D(\theta) > 0$ termed as tumble), and search for ways out of neutral media (avoid being at positions where $J_D(\theta)=0$).

At the end of the required number of chemotaxis steps an assessment is made about the health of the bacteria by sorting them in the ascending order. Half of the healthy bacteria is replicated by assigning the same location and the other half is eliminated. This operation constitutes the reproduction step.

After the end of the desired number of reproduction steps, each bacterium may be eliminated or dispersed with some probability. This step is known as Elimination and dispersal and is meant to shake up the bacteria so as to move them to better locations.

The initialization for the Bacterial Foraging algorithm is done as per the guidelines in [39]

1. Set the number of bacteria $B=50$.

2. The number of parameters w to be optimized are 2: T_U, T_V .
3. Swimming length $N_s=4$.
4. N_c , the number of iterations in a chemotactic loop is set to 100.
5. N_{re} , the number of reproduction steps is set to 2.
6. N_{ed} , the number of elimination and dispersal events is set to 2.
7. The probability p_{ed} that each bacterium will be eliminated/dispersed is set to 0.25.
8. Location of each bacterium $L(w, B, N_c, N_{re}, N_{ed})$.

3.4. C. Results of color segmentation

3.4.1. Segmentation evaluation indices

The quality of the segmentation is generally judged by two types of indices: the *goodness methods* such as Liu's F -measure which ascertains the color difference in the CIELAB color space and also penalizes the formation of large number of segments, and the *discrepancy methods* which ascertain the quality with respect to some reference result like ground truth images for example the RAND index. The above two types of quality measures are used together to judge the efficiency and practicality of the proposed algorithm.

1. *Liu's Evaluation Measure (F)*: The performance of color segmentation is evaluated using Liu and Yang's [41] evaluation function F :

$$F(I) = \frac{1}{1000(N_1 \times N_2)} \sqrt{G} \sum_{i=1}^G \frac{e_i^2}{\sqrt{A_i}} \quad (17)$$

where I is the segmented image and $N_1 \times N_2$ is the image size, G is the number of regions of the segmented image, A_i is the area and e_i is the average color error of the i th region where e_i is defined as the sum of Euclidean distances between the $\{a^*, b^*\}$ color vector of the pixels of region i and the color centroid attributed to region i in the segmented image. The smaller the value of $F(I)$ the better the segmentation result. We choose Liu's F -factor as one of our evaluation criteria since it gives an accurate measure of the color differencing achieved by the segmentation algorithm and at the same time penalizes large number of regions formed.

2. (a) *Probabilistic RAND index (PR)*: The PR index is a generalization of the RAND index [42] introduced by Unnikrishnan et al. in [43]. It allows a comparison of the test segmentation with multiple ground truth images through soft non-uniform weighting of pixel pairs as a function of the variability in the ground truth sets.

Suppose each human k provides information about the segmentation in the form of binary numbers $\prod(l_i^{S_k} = l_j^{S_k})$ for each pair of pixels (x_i, x_j) . The set of all perceptually correct segmentations defines a Bernoulli distribution giving a random variable with the expected value denoted as h_{ij} . The Probabilistic RAND index (PR) is then defined as

$$PR(S_{test}, \{S_k\}) = \frac{1}{(N/2)} \sum_{i < j} [m_{ij} h_{ij} + (1-m_{ij})(1-h_{ij})] \quad (18)$$

where m_{ij} denotes the event of a pair of pixels i and j having the same label in the test image S_{test} :

$$m_{ij} = \prod(l_i^{S_{test}} = l_j^{S_{test}}) \quad (19)$$

This measure takes values [0,1], where 0 means no similarities between S_{test} and $\{S_1, S_2, \dots, S_K\}$, and 1 means all segmentations are identical.

2. (b) *Normalized Probabilistic RAND index (NPR)*: The Normalized PR index by Unnikrishnan et al. in [12], is an excellent means of

qualitative comparison among image segmentation algorithms. Once the segmentation of all the test images for all the algorithms being compared has been compiled the Normalized PR index is calculated so that a global measure is possible.

$$\text{Normalized PR} = \frac{\text{PR-Expected PR}}{\text{Maximum PR-Expected PR}} \quad (20)$$

The above equation assures that the expected value of normalized index is zero providing a wider range. The maximum value of PR, Maximum PR , in (20) is taken as 1.

3.4.2. Color segmentation results

In this section experimental results are presented to prove the effectiveness of the proposed color segmentation algorithm on the natural images. For these results MATLAB (ver.7.9) software is run on a Pentium-IV 1.4 GHz PC. All images are digitized to 24 bits per pixel in the RGB format. Since the distance between any two points in the RGB space is not proportional to their color difference, transformation from the RGB space to a uniform color space: CIELAB [31] is performed. The vector $\{a^*, b^*\}$ of CIELAB color space contains the total chrominance color information of pixels and is the feature space for our color segmentation experiments. The vector $\{L^*\}$ or luminance vector which decides the darkness or fairness of the image segments is discarded in the clustering process to ensure that the illumination effects do not affect the segmentation process. It is observed that the FCCI algorithm yields highly crisp values of object membership function u_{ci} (close to 0 and 1). On the other hand the feature membership values v_{cj} are highly fuzzy (close to 0.5) due to averaging over the entire dataset. The v_{cj} values however are accentuated by the high values of parameter T_V ($\approx 10^8$) in Eq. (4) creating a considerable influence in the computation of u_{ci} , eventually leading to crisp values of u_{ci} after the iterative procedure. This helps in crisp classification during the defuzzification process.

A set of 100 test images is taken from the Berkeley segmentation database [44,45] along with 5–7 ground truth segmentations available for each image in the database for the evaluation of the results. The size of each image is either 321×481 or 481×321 and the average time taken by the FCCI algorithm for each image is approximately 35 s. The segmentation of all 100 images by the proposed FCCI algorithm is shown in Fig. 2, with the edges superimposed on original images. The corresponding graphs for Liu's F -factor and the Probabilistic RAND index (PR) is shown in Fig. 3 for 100 images bestowing excellent values for both segmentation evaluation measures. The results show a good match with human ground truth segmentations as indicated by a high value of Probabilistic RAND index (PR), and also efficient color differentiation as indicated by a low value of Liu's evaluation measure F . The number of clusters is determined from the first local minima in the cluster validity S graph (normally < 7 clusters for our experiments) as demonstrated by the example shown in Fig. 4.

Some observations made from the results obtained are as follows:

1. *Tradeoff between color differencing and human perception*: in the case of images with distinct colors (Fig. 5) there is an excellent correspondence with human perception (high NPR) but the color differentiation is not so good (high Liu's F -factor). In the case of images with indistinct colors (Fig. 6), very good color difference is observed (low Liu's F -factor) but the results appear to be over-segmented and hence NPR value is relatively less. The proposed technique therefore maintains a good tradeoff between the two segmentation evaluation measures.
2. *Sensitivity to parameters*: the algorithm is found to be more sensitive to the values of T_U than T_V since the values of u_{ci}

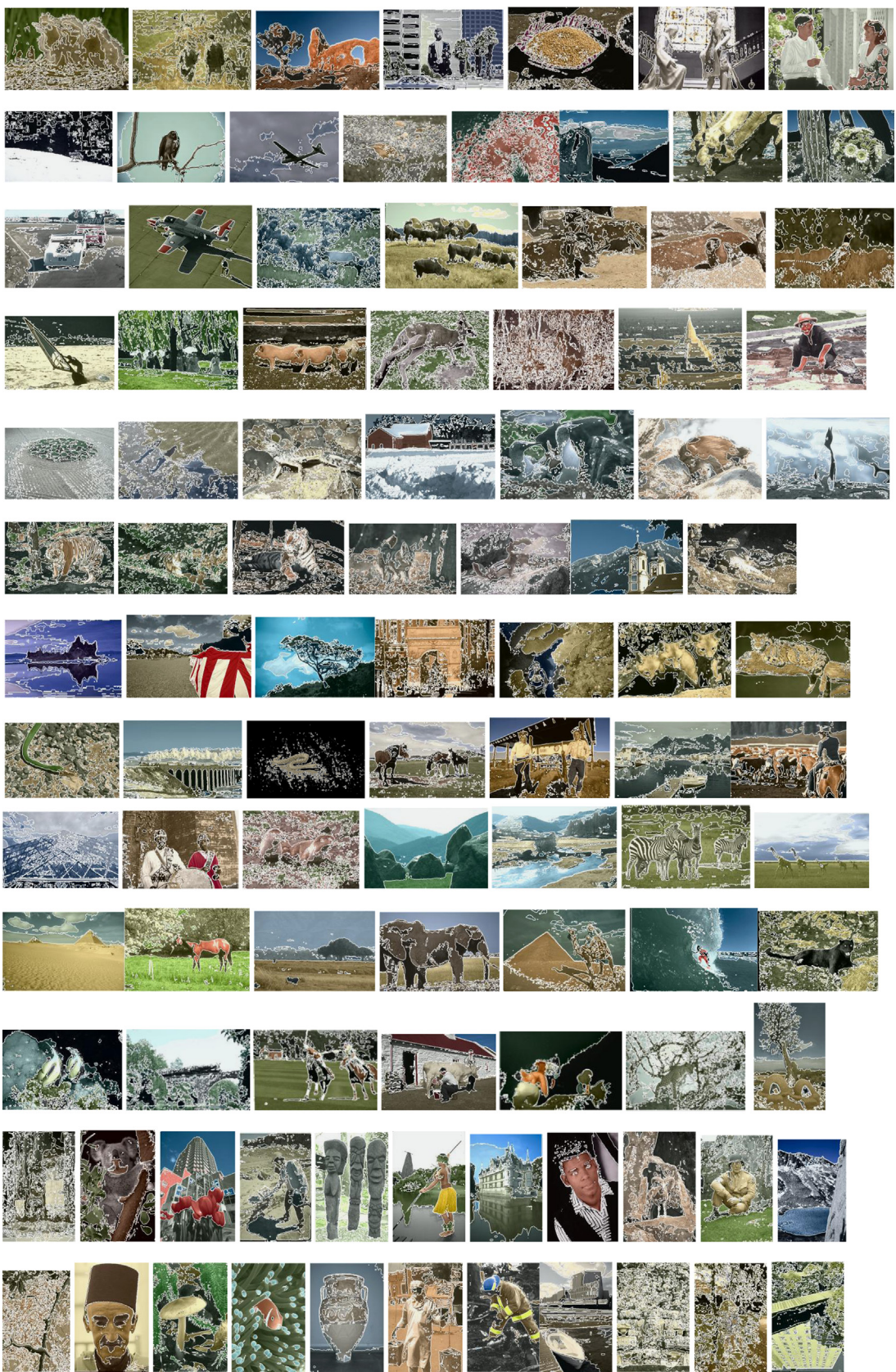


Fig. 2. Color Segmentation Results of 100 test images from Berkeley segmentation database [44] by the proposed method. (For interpretation of the references to color in this figure legend, the reader is referred to the web version of this article.)

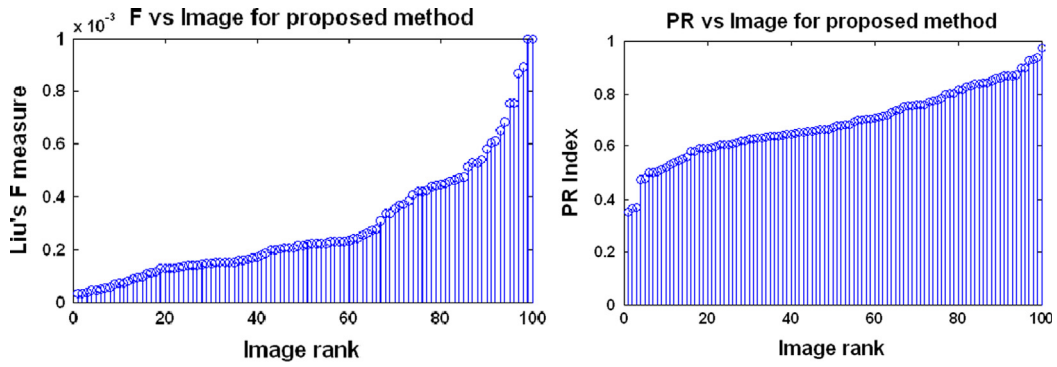


Fig. 3. Liu's F-measure and PR index in the increasing order for segmentations of 100 test images from Berkeley dataset [44] by the proposed method.

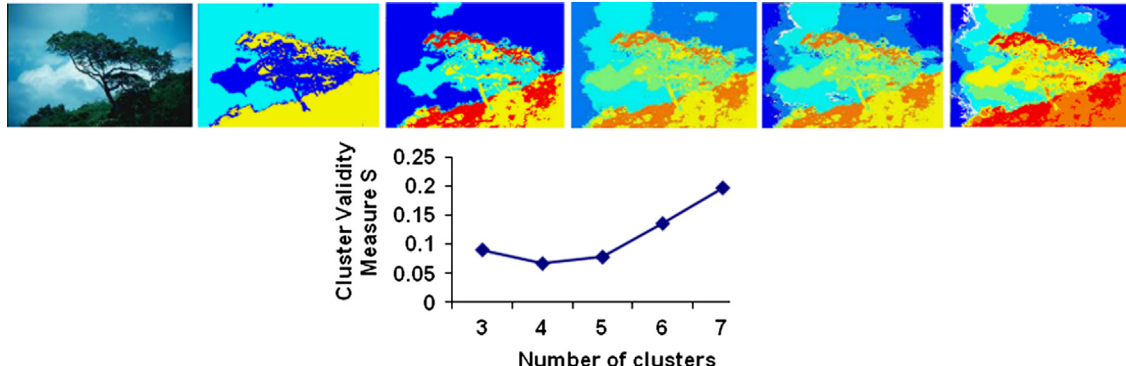


Fig. 4. Original image and Segmentation results (from left to right and top to bottom) of “Tree” image and the corresponding Clustering validity graph as the number of clusters c is varied from 3 to 7. Corresponding values of NPR and Liu's F-factor are: c: 3, 4, 5, 6, 7; NPR: 0.5519, 0.5203, 0.1314, -0.213, -0.1332; F: 0.00044, 0.000347, 0.000322, 0.000332, 0.000342. Number of clusters is aptly determined to be C=4 (from the first local minima in the graph) as it results in the most optimum combination of NPR and Liu's F-factor.



Fig. 5. Example segmentations of images with distinct colors—NPR(from left to right): 0.6065, 0.7962, 0.8007, 0.9213; F(from left to right): 0.00047, 0.000138, 0.000134, 0.000085. (For interpretation of the references to color in this figure legend, the reader is referred to the web version of this article.)

obtained are very crisp and a careful choice of T_U in (4) is required for the algorithm to converge. Replacing the Bacterial Foraging optimization by the Genetic algorithm in our experiments results in a large computational overhead with an initial population of 100 chromosomes required for acceptable results, while Bacterial Foraging starts giving good results for the initial population of 8 bacteria, thereby, significantly reducing the computational overhead.

The value of T_U in our experiments is found to range from 1–30 for different images with values close to 1 for images with non-distinct colors (Fig. 6) and higher values for visually distinct colors (Fig. 5). The valid values of T_V ranges widely from 10^6 – 10^8 and do not have a major impact on the resulting clusters since its only function is to contribute to the computation of u_{ci} by scaling v_{cj} .

3. Complex illumination Patterns: the algorithm is able to segment natural scenes containing non-uniform illumination efficiently

(Fig. 7(a)) by segregating shadows from sunlit portions thus agreeing with human perception. However in the cases where the shadows tend to merge with the colors in the scene (Fig. 7(b)) result tends to look over-segmented in spite of very good color differencing (low F).

4. Under-segmentation: only in rare cases (1 out of 100) the algorithm fails to segregate extremely indistinct colors as demonstrated by the under-segmented result in Fig. 8 due to formation of highly fuzzy clusters.

3.4.3. Comparisons with other methods

The proposed color segmentation technique is compared with some well known methods in literature for unsupervised color segmentation: Fuzzy C-Means (FCM) [22,37], Normalized Graph-Cut (N-CUT) Method [10], Gaussian Mixture model (GMM) [8] and

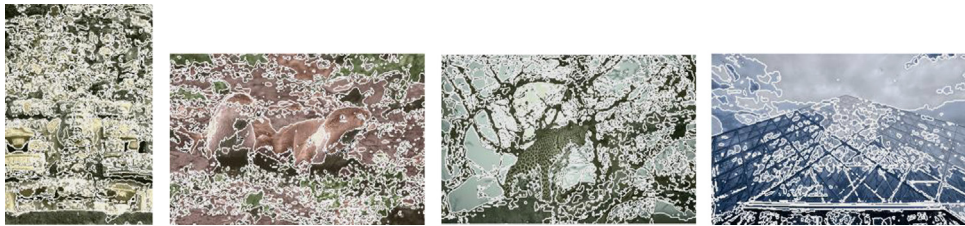


Fig. 6. Example segmentations of images with indistinct/similar colors—NPR (from left to right): -0.284, -0.391, -0.334, -0.098; F (from left to right): 0.000053, 0.00023, 0.000057, 0.0000701. (For interpretation of the references to color in this figure legend, the reader is referred to the web version of this article.)

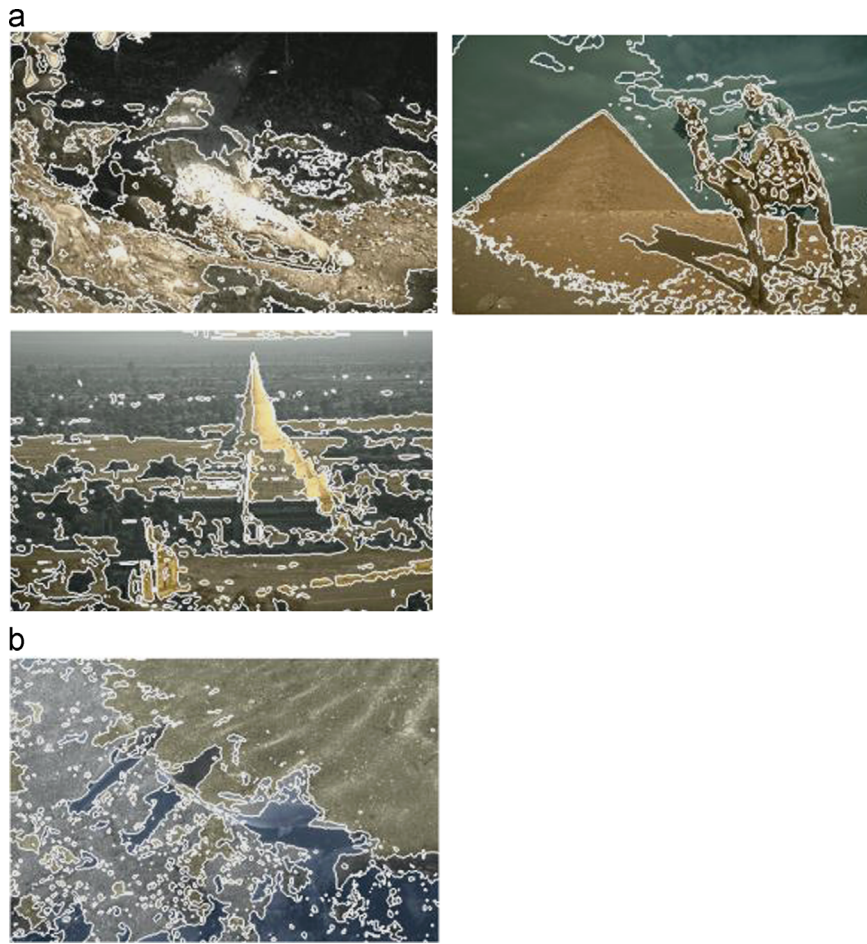


Fig. 7. Example segmentations with shadows and non-uniform illumination. NPR (from left to right): (a) -0.301, 0.314, -0.022 and (b) -0.7609; F (from left to right): (a) 0.00025, 0.00023, 0.00026 and (b) 0.00015.

Mean-Shift (MS) [9] segmentation methods. The CIELAB color space is used for all the comparisons. While both mean shift and NCUT graph based method are popular feature space clustering methods, FCM is chosen since it is a widely popular fuzzy clustering method for image segmentation. The parameters for FCM algorithm used in our experiments are: index of fuzziness $m=2$, maximum error limit $\epsilon=10^{-2}$, maximum iteration = 200. Normalized Cuts graph based segmentation method uses eigenvector techniques to obtain graph partitions. It finds minimum cuts in a graph while minimizing the similarity between different patches. GMM models the color features as a mixture of Gaussian kernels using Expectation Maximization algorithm for estimation of parameters of the Gaussian mixture and is a popular method for image segmentation and retrieval. Figs. 9 and 10 show the graphs for F and NPR indices for the 100 test images from the Berkeley Segmentation Dataset in the form of histograms for the five methods. It is observed from the graphs that the proposed FCCI

algorithm provides the most optimum combination of the lowest values of F -measure (of the order of 10^{-4}) and sufficiently high values of NPR index among all the five methods proving the efficiency of the proposed color segmentation algorithm by striking a neat balance between color differencing and human perception standards.

Fig. 11 shows the color segmented results of the five methods for six randomly selected test images from the Berkeley Segmentation Dataset namely: 'Mud-Huts', 'Plane', 'Eagle', 'Building', 'Wolf', 'Tree'. The corresponding F and NPR segmentation evaluation indices are listed in Table 1 depicting the lowest values of F for the proposed method as compared to all other methods. The NPR readings are also observed from Table 1, to be overall best for the proposed method though the Mean-Shift algorithm performs better for 'Plane' image. It is observed from the segmentation results in Fig. 11(b) that the proposed method FCCI forms well defined and interpretable clusters even when the color difference

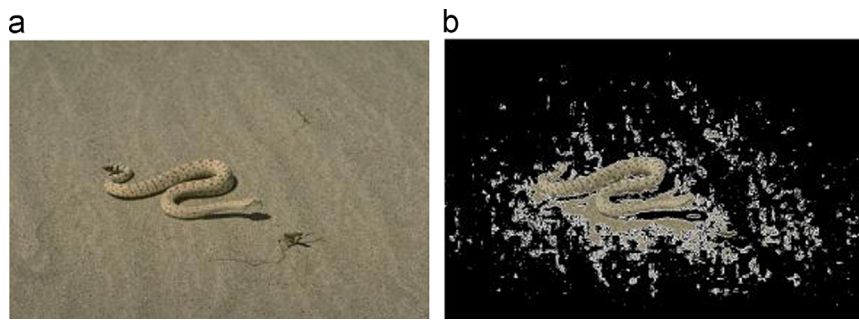


Fig. 8. (a)Original image and (b) under-segmented result.

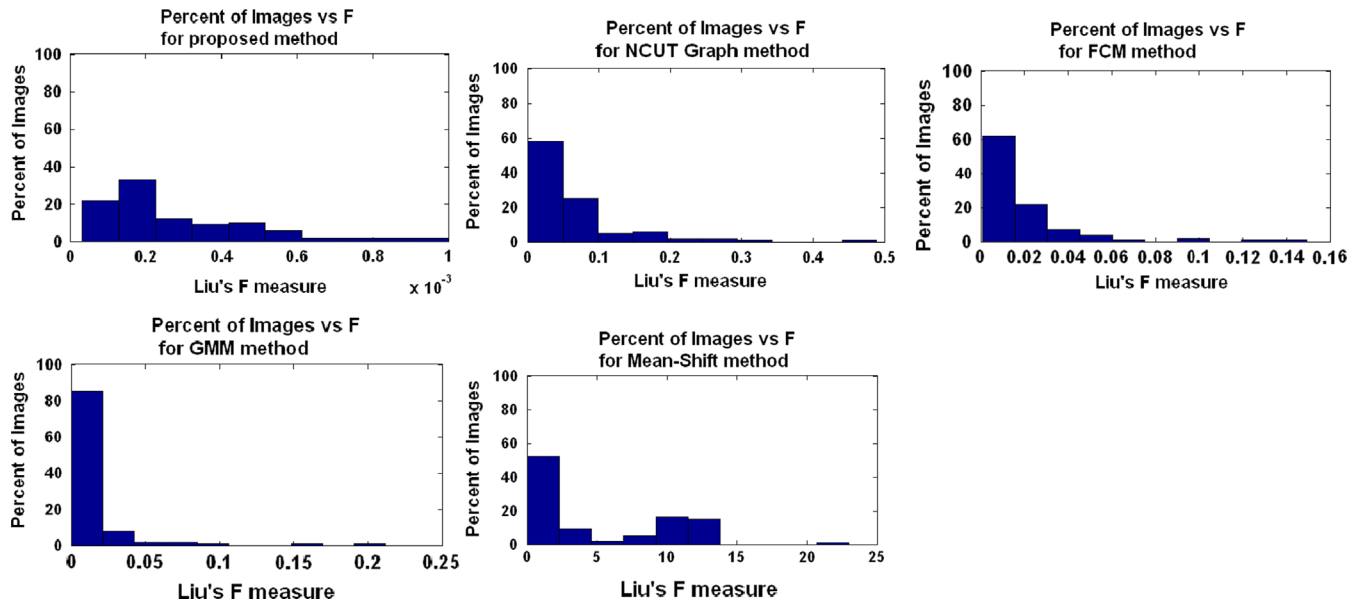


Fig. 9. Histograms of Liu's F -measure achieved for individual images for the proposed method, NCUT Graph based method, FCM, GMM, Mean-shift segmentation methods.

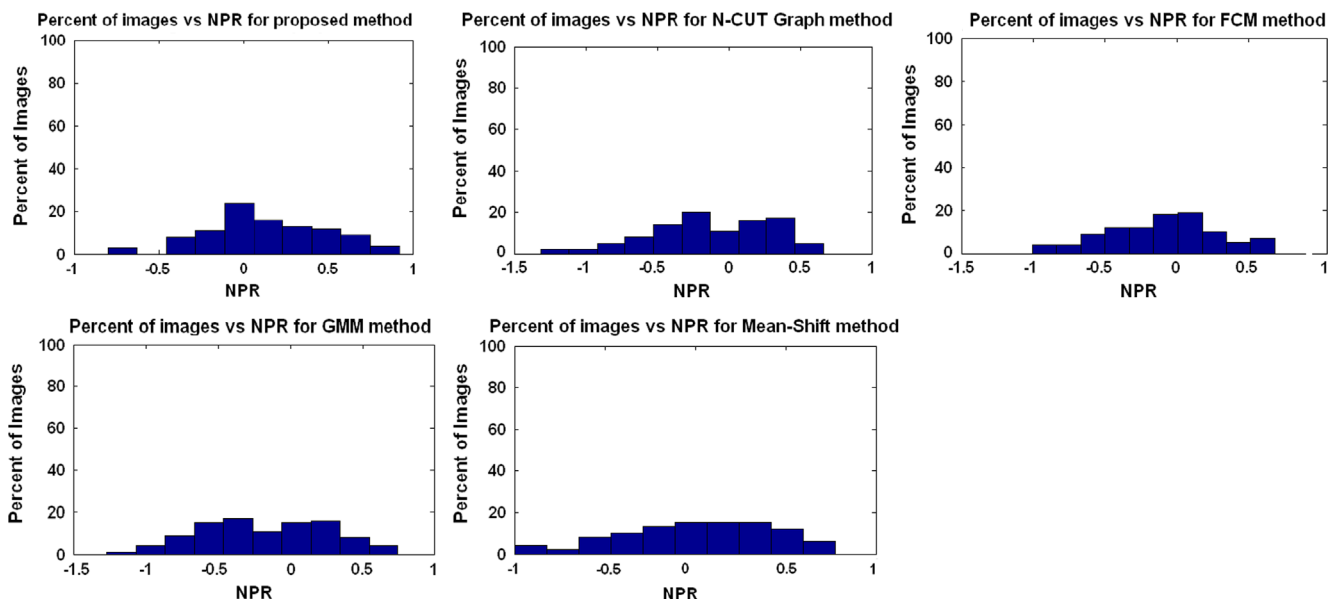


Fig. 10. Histograms of NRP Index achieved for individual images for the proposed method, NCUT Graph based method, FCM, GMM, Mean-shift segmentation methods.

between two regions is not too distinct as in the case of ‘Wolf’ image. The proposed technique is efficient in segmenting out uniform color regions and gives less fake boundaries as observed

in the case of ‘Building’ image in Fig. 11(b) where the windows of the building are nicely segmented out visually as compared to other methods. An important factor that gives FCCI an edge over

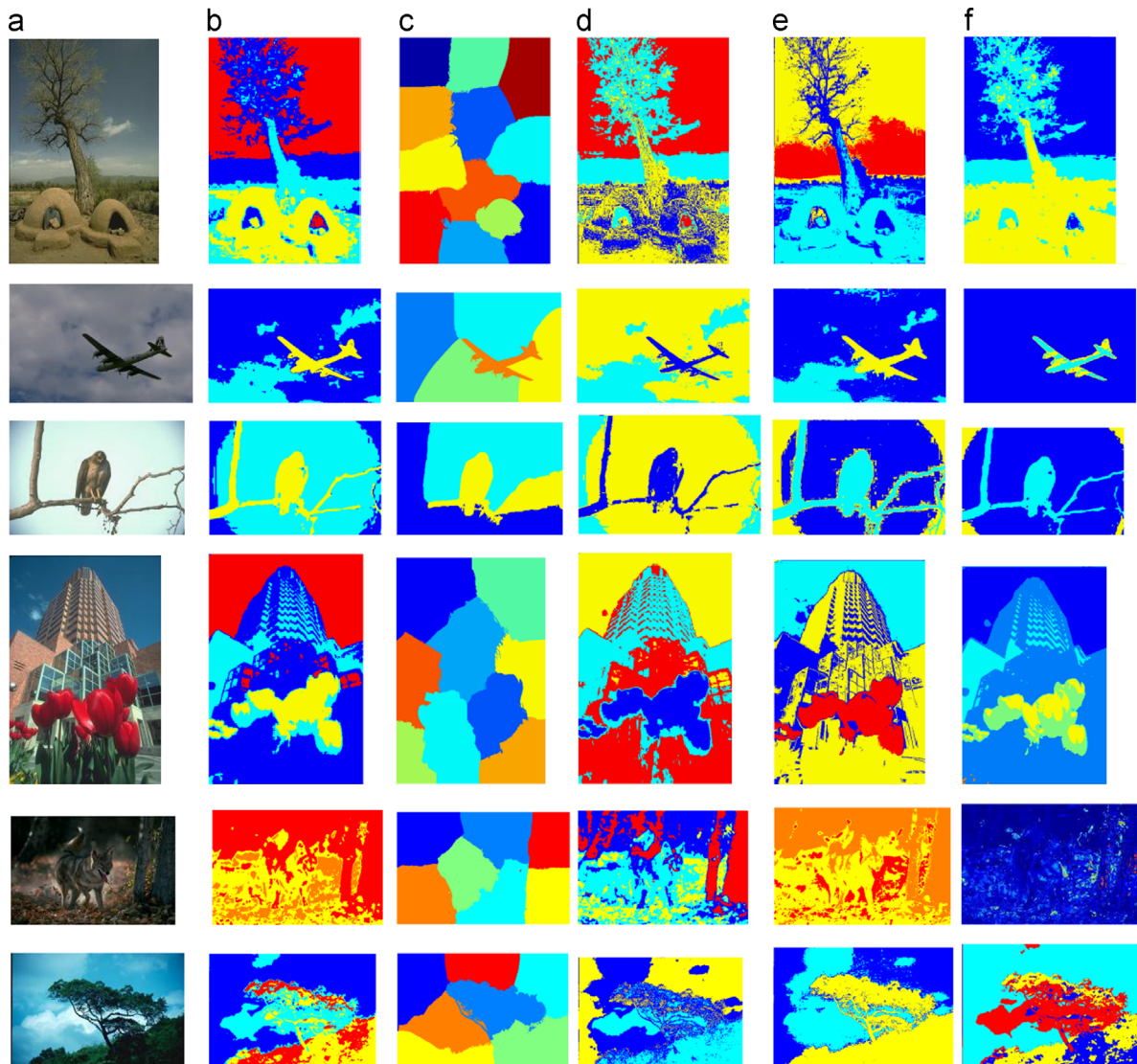


Fig. 11. Color segmentation results (a) Original images from Berkeley segmentation database [57] : 'Mud-Huts', 'Plane', 'Eagle', 'Building', 'Wolf', 'Tree' (b) Proposed method [(from top to bottom): $T_U = \{10.96, 1.15, 2.05, 9.52, 4.81, 11.79\}$, $T_V = 10^8$] (c) N-CUT (d) FCM (e) GMM (f) Mean Shift segmentations [Space Bandwidth $h_s = 15$, Color bandwidth h_r (from top to bottom): $\{7, 3, 4, 10, 1, 8\}$]. (For interpretation of the references to color in this figure legend, the reader is referred to the web version of this article.)

Table 1

Liu's F -measure and normalized probabilistic RAND index for the six test images: 'Mud-Huts', 'Plane', 'Eagle', 'Building', 'Wolf', 'Tree'.

	Mud-Huts		Plane		Eagle		Building		Wolf		Tree	
	F	NPR	F	NPR	F	NPR	F	NPR	F	NPR	F	NPR
Proposedmethod	0.000128	0.3324	0.000045	0.425	0.000142	0.4466	0.0010	0.3496	0.000147	-0.0979	0.000447	0.5203
N-CUT	0.060	0.1904	0.0054	-0.4135	0.0020	0.4419	0.2506	0.2653	0.0100	-0.4611	0.0449	0.049
FCM	0.0154	0.2514	0.0028	0.2234	0.0061	0.4097	0.0909	0.2403	0.0054	-0.6522	0.0086	0.09
GMM	0.0131	0.2237	0.0035	0.1815	0.0034	0.3476	0.0874	0.135	0.0034	-0.6996	0.0084	0.3069
Meanshift	0.0075	0.3146	0.0122	0.6562	0.3013	0.5353	1.2487	0.3346	23.5	-0.4861	0.0225	0.3734

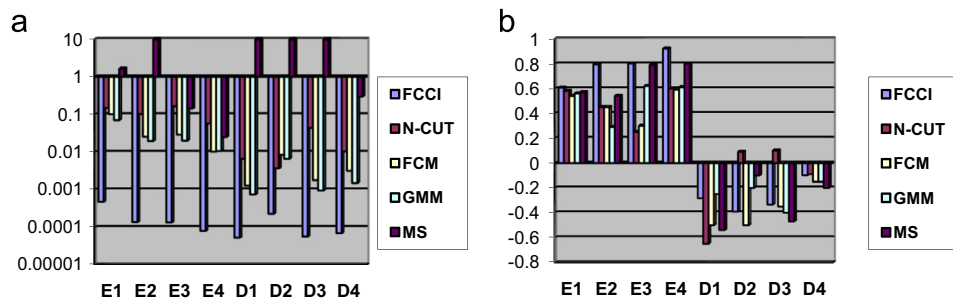


Fig. 12. The plots for (a) F -value (logarithmic scale) and (b) NPR readings for 4 easy (E1 to E4) images (from Fig. 5) and 4 difficult (D1 to D4) images (from Fig. 6) are shown below.

FCM clustering technique is the reduced time complexity. The time required by FCM for clustering is 10–15 min while the proposed algorithm hardly takes 1 min for the same. How fuzzy co-clustering scores over fuzzy clustering can be observed by comparing the segmentations of the proposed method (Fig. 11(b)) with that of FCM (Fig. 11(d)). The criterion for choosing number of clusters is the same as that for the proposed method (from the local minima in the clustering validity graph). As seen in the ‘Tree’ image co-clustering forms distinct and correct clusters with

criteria being maximum separation between clusters/colors. Thus the green foliage and the blue sky being of distinct colors are grouped into separate clusters by the proposed method whereas in FCM, the parts of sky/clouds are clustered together with green foliage. FCM also suffers from the problem of outliers as observed from the pigmented segmentations in the ‘Mud-Huts’ example in Fig. 11(d). The co-clustering results are improved because of the grading/relevance factor (feature membership function) assigned to each of the color feature (a^*, b^*) with respect to a particular

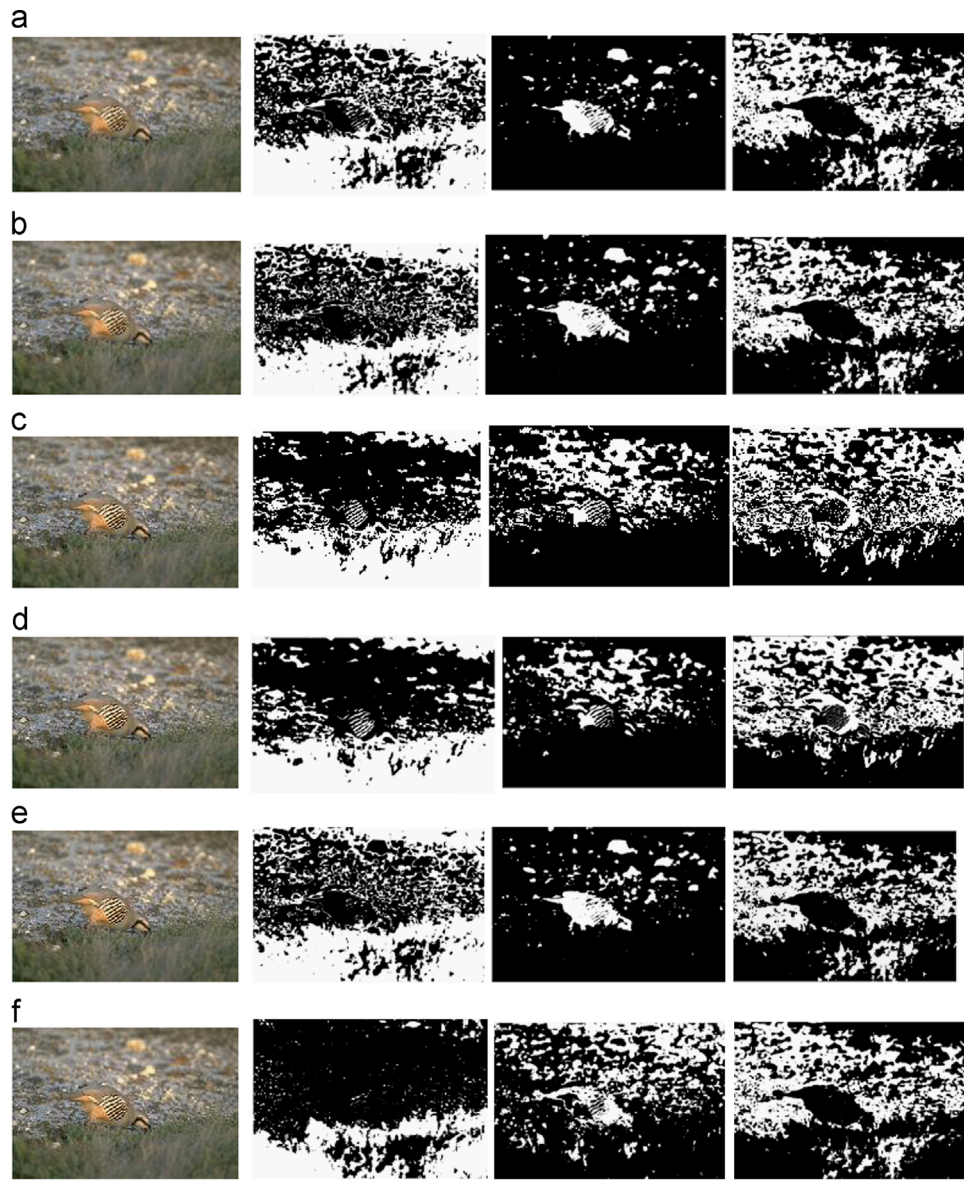


Fig. 13. The comparison of fuzzy clustering results (with the best values in bold) on the ‘Bird’ image for three clusters (a) FCCI (b) FCM (c) Histogram Weighted FCM (d) Spatially Weighted FCM (e) PFCM (f) OSFCM (g) Segmentation Evaluation results in terms of Mean Square Error (MSE), Region Homogeneity Test (RH) and Mean Square Error (MSE) in the presence of noise.

Clustering Evaluation Criteria	FCCI	FCM	HWFCM	SWFCM	PFCM	OSFCM
Average MSE of clusters (Accuracy of clustering)	34.7	34.6	187	207	34.6	52.7046
Total Number of regions segmented (Semantic meaning of clusters)	530	646	673	822	648	940
Region Homogeneity test for $u>0.5$ (inlier test)	100%	95%	99.9%	99.87%	95%	89.04%
Average MSE of clusters with added noise (outlier test)	300	326	184	194	216	660

cluster which leads to correct evaluation of clusters and also solves the problem of outliers. The N-CUT Graph based method does not give a very good correctness with respect to human ground truth images as compared to the proposed method and mean shift method. Also it tends to segregate uniform color regions into large chunks. GMM by Expectation Maximization algorithm is an unsupervised technique resulting in blob like segments. It classifies the entire tree and green foliage of the example 'Tree' in Fig. 11(e) into 1 segment performing well with respect to human evaluation but poorly for color difference between regions. Moreover, the resulting blobs contain no internal details as demonstrated in the blobs formed in 'Eagle' image in Fig. 11(e). The mean shift algorithm performs well corresponding to human ground truths as indicated by a high value of NPR (example—'Plane' image in Fig. 11(f)). However it fails in the absence of any dominant colors in the scene as seen in the example of 'Wolf' image where the colors are visually indistinct. The Liu's *F*-measure values are found to be generally high in the case of both mean shift and N-CUT graph based algorithms. Also the mean shift method is very sensitive to its color bandwidth parameter h_r with a slight change causing large changes in granularity of segmentation. The h_r values for the test images are in the range 1–15 while the space bandwidth is $h_s=15$. Though some feature weighted clustering algorithms have been proposed in the past [46] and were applied for image segmentation problems [47], they do not incorporate a separate feature membership to be independently updated in each iteration along with pixel memberships and cluster centroids. Fig. 12 shows the comparison (*F* and NPR values) between the five methods for the mix of easy and difficult images in Figs. 5 and 6 respectively taken in the same order. The results affirm that *F*-values are minimum for FCCI for all images, a fact already established from the graphs in Fig. 9, while NPR values are highest

for FCCI for all the easy images E1 to E4 and most of the difficult images except for the D2 difficult image for which NCUT, GMM and Mean Shift yield better results. In Fig. 13 we compare the segmentations using some recent fuzzy clustering algorithms apart from FCM namely Spatially weighted FCM [48], Histogram weighted FCM [49], Possibilistic FCM [50] and Orientation sensitive FCM (OSFCM) [51] on an example image 'Bird' containing three main clusters, the bird, the stones and the grass. The experimental parameters of these algorithms are summarized in Table 2. The results in Fig. 13 indicate that FCCI provides the most optimum segmentation with respect to human evaluation of the scene and is equivalent to FCM in terms of accuracy of the clusters formed. FCM and FCCI form the most visually acceptable clusters of the scene segmenting out the bird nicely in Cluster 2. Hence the reason that FCM among all the existing fuzzy clustering algorithms is most popular for image segmentation purpose. FCCI yields the cleaner image of the two (with lesser number of regions as compared to FCM as seen in Fig. 13) complying more with human perception of the scene.

The inlier or bridge pixels are properly clustered by FCCI as compared to all other clustering algorithms as indicated by the region homogeneity tests (criteria being $u_{ci} > 0.5$), though the outlier problem of FCM persists. The inlier pixels are defined as those that are equidistant from all centroids and have a membership of 0.5 to all clusters as a result. Since FCCI computes feature memberships as well which evaluates the relationship of a cluster to a feature, it is taken into account the feature value distribution of the inlier to compute its membership to a cluster. However the outlier points or noise pixels are a problem since for these data points the algorithm behaves like FCM and is sensitive though some marginal improvement is noticed from the Table in Fig. 13. Table 3 evaluates the memberships obtained from

Table 2
Experimental parameters of the fuzzy clustering algorithms being compared.

Algorithm	Parameters	Parameter optimization technique	Clustering data (from CIEL*a*b* color space)	Computational complexity*	Dissimilarity measure*	Average number of iterations needed for convergence (EL=0.01)	Average execution time
Fuzzy co-clustering algorithm for images (FCC1)	T_u, T_v	<i>Bacterial foraging</i>	a^*, b^*	<i>Object membership u (CxN)</i> <i>Feature membership v (CxK)</i> <i>Centroid p (CxK)</i> <i>Object membership u (CxN)</i> <i>Centroid p (CxK)</i> <i>Object membership u (CxN)</i> <i>Centroid p (Cx1)</i> <i>Object membership u (CxN)</i> <i>Centroid p (Cx1)</i> <i>Object membership u (CxN)</i> <i>Typicality T (CxN)</i> <i>Centroid p (Cx1)</i> <i>Object membership u (CxN)</i> <i>Centroid p (Cx1)</i>	$v_{cj}D_{cij}$ (CxNxK)	33	(with 8 bacteria) < 1 min
Fuzzy C-means algorithm (FCM)	$m=2$	<i>none</i>	a^*, b^*	<i>Object membership u (CxN)</i> <i>Centroid p (CxK)</i> <i>Object membership u (CxN)</i> <i>Centroid p (Cx1)</i> <i>Object membership u (CxN)</i> <i>Centroid p (Cx1)</i> <i>Object membership u (CxN)</i> <i>Centroid p (Cx1)</i> <i>Object membership u (CxN)</i> <i>Centroid p (Cx1)</i>	D_{ci} (CxN)	27	10–15 min
Histogram weighted FCM (HWFCM)	$m=2$	<i>none</i>	L^*	<i>Object membership u (GLxN)</i> <i>Centroid p (Cx1)</i> <i>Object membership u (CxN)</i> <i>Centroid p (Cx1)</i> <i>Object membership u (CxN)</i> <i>Centroid p (Cx1)</i> <i>Object membership u (CxN)</i> <i>Centroid p (Cx1)</i>	D_{ci} (CxN)	61	10 s
Spatially weighted FCM (SWFCM)	$m=2$	<i>none</i>	L^*	<i>Object membership u (CxN)</i> <i>Centroid p (Cx1)</i> <i>Object membership u (CxN)</i> <i>Centroid p (Cx1)</i> <i>Object membership u (CxN)</i> <i>Centroid p (Cx1)</i> <i>Object membership u (CxN)</i> <i>Centroid p (Cx1)</i>	D_{ci} (CxN)	100	20 s
Possibilistic FCM (PFCM)	$m=2, \eta=1.2, a=b=1$	<i>none</i>	a^*, b^*	<i>Object membership u (CxN)</i> <i>Typicality T (CxN)</i> <i>Centroid p (Cx1)</i> <i>Object membership u (CxN)</i> <i>Centroid p (Cx1)</i>	D_{ci} (CxN)	33	20 min
OSFCM	$m=2$	<i>none</i>	a^*, b^*	<i>Object membership u (CxN)</i> <i>Centroid p (Cx1)</i>	D_{ci} (CxN)	10	20 min

(*where number of clusters $c=1$ to C , number of data points $i=1:N$, number of features $j=1:K$, number of Gray levels $gl=1$ to GL with $GL \ll N$, and $D=\|\cdot\|_2$, the Euclidean distance norm)

Table 3

Clustering comparison of FCCI, FCM, PFCM—response to inliers and normal data points.

S. no.	Fuzzy Co-clustering algorithm for images (FCCI) (Membership values) ($T_U=0.96$, $T_V=9 \times 10^7$)			Fuzzy C-means algorithm (FCM) (Membership values) ($m=2$)	Possibilistic FCM (PFCM) (Typicality values) ($m=2, \eta=2, a=b=1$)		
	Data	x	y	U_1, U_2	U_1, U_2	T_1, T_2	
1		-5	0	1,0	0.936, 0.06	0.621, 0.113	
2		-3.34	1.67	1,0	0.97, 0.03	0.801, 0.165	
3		-3.34	0	1,0	0.99, 0.01	0.953, 0.171	
4		-3.34	-1.67	1,0	0.9, 0.1	0.642, 0.157	
5		-1.67	0	1,0	0.92, 0.08	0.840, 0.278	
6		-1.67	0	0,1	0.08, 0.92	0.278, 0.840	
7		-3.34	1.67	0,1	0.03, 0.97	0.165, 0.801	
8		-3.34	0	0,1	0.01, 0.99	0.171, 0.953	
9		-3.34	-1.67	0,1	0.1, 0.9	0.157, 0.642	
10		5	0	0,1	0.06, 0.94	0.113, 0.621	
11 (Inlier)		0	0	0.50031, 0.4997	0.5, 0.5	0.49, 0.49	
Cluster centers (Centroids)				-3.03 3.03	0 0	-2.99 2.29	0 0

FCCI, FCM and PFCM algorithms for the X_{11} dataset $\{X_{10} \cup \text{(inlier)}\}$ in [50] where X_{10} contains 10 two dimensional data points. The results are found to be best for the proposed FCCI algorithm in terms of crisp values of memberships (1,0) obtained and the definitive values of inlier memberships that is indicative of the clusters ($u_{ci} > 0.5$) to which they belong to. The only shortcoming of FCCI clustering is the response to the outliers which need to be minimized.

4. Conclusions

In this paper, the Fuzzy co-clustering approach based on the simultaneous clustering of both object and feature memberships is used for the color segmentation of natural images. A new objective function is formulated and the update rules are derived. The new algorithm (FCCI) is tried for color segmentation on 100 test images from the Berkeley segmentation dataset yielding precise segmentation. The color vectors $\{a^*, b^*\}$ of CIELAB color space are the feature variables for the color segmentation algorithm. The performance is evaluated on the basis of Liu's Function F , and the Normalized Probabilistic RAND (NPR) index. The number of clusters is determined from the first local minima of Xie and Beni's cluster validity curve and is found to produce apt results (low F and high NPR). The proposed method produces accurate color differencing and at the same time adheres to the human perception in segmenting the natural scenes with non-uniform illumination and shading. It is also compared with some of the existing color segmentation techniques and is found to outperform them. The future scope of this work lies in improving the image segmentation in the presence of outliers and exploring other evolutionary algorithms for speedy solutions of the two parameters involved.

Appendix A

The proof of convergence of the FCCI algorithm is shown below:

Theorem 1. The updated values of u_{ci} given by Eq.(9) never increase the objective function in every iteration.

Proof. Consider the objective function as a function of u_{ci} alone.

$$J_{FCCI}(U) = \sum_{c=1}^C \sum_{i=1}^N \sum_{j=1}^K u_{ci} v_{cj} D_{cij} + T_U \sum_{c=1}^C \sum_{i=1}^N u_{ci} \log u_{ci} + \text{constant} \quad (31)$$

where, $\text{constant} = T_V \sum_{c=1}^C \sum_{j=1}^K v_{cj} \log v_{cj}$

Also, the product $v_{cj} D_{cij}$ may be considered as constant. To prove **Theorem 1** we have to prove that U^* , i.e the updated values of u_{ci} given by Eq. (9) are the local minima of the objective function $J_{FCCI}(U^*)$ provided that the constraints in (5) and (6) are satisfied. For this we need to prove that the Hessian matrix $\Delta^2 J_{FCCI}(U^*)$ is positive definite.

$$\Delta^2 J_{FCCI}(U) = \begin{bmatrix} \frac{\partial^2 J_{FCCI}(U)}{\partial u_{11} \partial u_{11}} & \dots & \frac{\partial^2 J_{FCCI}(U)}{\partial u_{11} \partial u_{CN}} \\ \vdots & \ddots & \vdots \\ \frac{\partial^2 J_{FCCI}(U)}{\partial u_{CN} \partial u_{11}} & \dots & \frac{\partial^2 J_{FCCI}(U)}{\partial u_{CN} \partial u_{CN}} \end{bmatrix} = \begin{bmatrix} \frac{T_U}{u_{11}} & \dots & 0 \\ \vdots & \ddots & \vdots \\ 0 & \dots & \frac{T_U}{u_{CN}} \end{bmatrix} \quad (32)$$

At U^* , $u_{ci} \geq 0$ and T_U is always assigned a positive value. Therefore the Hessian matrix $\Delta^2 J_{FCCI}(U^*)$ is positive definite. We have proved the first necessary condition $(\partial J_{FCCI}(u_{ci}) / \partial u_{ci}) = 0$ and the second sufficient condition: $\Delta^2 J_{FCCI}(U^*)$ is positive definite. Therefore u_{ci}^* updated is indeed a local minima of $J_{FCCI}(U)$ and it never increases the objective function value.

Theorem 2. For every iteration the updated values of v_{cj} given by Eq. (11) never increases the objective function. \square

Proof. Proof is similar to proof of **Theorem 1**.

Theorem 3. The following constraint is satisfied by J_{FCCI} in (4):

$$J_{FCCI} \geq T_U \times N \times \log \frac{1}{C} + T_V \times C \times \log \frac{1}{K}$$

Proof. Since the minimum value of u_{ci} and v_{cj} is 0, and $D_{cij} \geq 0$, the first term of J_{FCCI} reduces to

$$\sum_{c=1}^C \sum_{i=1}^N \sum_{j=1}^K u_{ci} v_{cj} D_{cij} \geq 0 \quad (33)$$

The second and third terms denote the entropy values and maximum value of entropy occurs when $u_{ci}=1/C$ and $v_{cj}=1/K$.

In view of these the point of minima is

$$J_{FCCI} \geq T_U \times N \times \log \frac{1}{C} + T_V \times C \times \log \frac{1}{K} \quad (34)$$

Corollary. *Theorems 1–2 prove that the updated equations of FCCI point to a local minima of the Objective function and Theorem 3 indicates the lower limit of J_{FCCI} .*

Appendix B

The CIELAB color space is obtained from the RGB color space by the following transformation:

$$\begin{bmatrix} X \\ Y \\ Z \end{bmatrix} = \begin{bmatrix} 0.490 & 0.310 & 0.200 \\ 0.177 & 0.813 & 0.011 \\ 0.000 & 0.010 & 0.990 \end{bmatrix} \begin{bmatrix} R \\ G \\ B \end{bmatrix} \quad (35)$$

The features of CIELAB are derived from

$$L^* = \begin{cases} 116(Y')^{1/3} - 16 & \text{if } Y' > 0.008856 \\ 903.3Y' & \text{otherwise} \end{cases} \quad (36)$$

$$a^* = 500[K1^{1/3} - K2^{1/3}] \quad (37)$$

$$b^* = 200[K2^{1/3} - K3^{1/3}] \quad (38)$$

where

$$K_i = \begin{cases} \phi_i & \text{if } \phi_i > 0.008856 \\ 7.787\phi_i + \frac{16}{116} & \text{otherwise} \end{cases} \quad \text{for } i = 1, 2, 3 \quad (39)$$

$$\phi_1 = X' = \frac{X}{X_0}, \phi_2 = Y' = \frac{Y}{Y_0}, \phi_3 = Z' = \frac{Z}{Z_0} \quad (40)$$

The X_0 , Y_0 and Z_0 are the values of X, Y, Z for the reference white, respectively. The reference white is defined as $\{R=G=B=255\}$.

References

- [1] Y.C. Ohta, T. Kanade, T. Sakai, Color information for region segmentation, *Comput. Graphics Image Process.* 133 (1980) 222–241.
- [2] Jayarammamurthy , S.N. and T.L.Huntsberger, Edge and region analysis using fuzzy sets, in: Proceedings of the IEEE Workshop on Language automation, June 1985, pp. 71–75.
- [3] P. Arbelaez, et al., From contours to regions: an empirical evaluation, *CVPR* (2009).
- [4] A. Tremeau, N. Borel, A region growing and merging algorithm to colour segmentation, *Pattern Recognition* 30 (7) (1997) 1191–1203.
- [5] S.C. Cheng, Region growing approach to color segmentation using 3-D clustering and relaxation labeling, *IEEE Trans. Vision Image Signal Process.* (2003) 270–276.
- [6] C.C. Kang, W.J. Wang, Fuzzy based seeded region growing for image segmentation, *NAFIPS* (2009).
- [7] M.R.F. Mukherjee, clustering for segmentation of color images, *Pattern Recognition Lett.* 23 (2002) 917–929.
- [8] C. Carson, S. Belongie, H. Greenspan, J. Malik, Blobworld: image segmentation using expectation maximization and its application to image querying, *IEEE Trans. Pattern Anal. Mach. Intell.* 24 (8) (2002).
- [9] D. Comaniciu, P. Meer, Mean-shift: a robust approach towards feature space analysis, *IEEE Trans. Pattern Anal. Mach. Intell.* 24 (5) (2002) 603–619.
- [10] J. Shi, J. Malik, Normalized cuts and image segmentation, *IEEE Trans. Pattern Anal. Mach. Intell.* 22 (8) (2000) 888–905.
- [11] P. Felzenszwalb, D. Huttenlocher, Efficient graph based image segmentation, *Int. J. Comput. Vision* 59 (2) (2004) 167–181.
- [12] R. Unnikrishnan, et al., Toward objective evaluation of image segmentation algorithms, *IEEE Trans. Pattern Anal. Mach. Intell.* 29 (6) (2007).
- [13] Arbib Uchiyama, Color image segmentation using competitive learning, *IEEE Trans. Pattern Anal. Mach. Intell.* 16 (12) (1994) 1197–1206.
- [14] Jiang Wang Cheng, Colour image segmentation :advances and prospects, *Pattern Recognition* 34 (2001) 1277–1294.
- [15] Soille Vincent, Watersheds in digital spaces, an efficient algorithm based on immersion simulations, *IEEE Trans. Pattern Anal. Mach. Intell.* 9 (1991) 735–744.
- [16] Tilton, D-Dimensional formulation and implementation of recursive hierarchical segmentation, NASA, Case no. GSC 15199-1.
- [17] Y. Deng, B.S. Manjunath, Unsupervised segmentation of color texture regions in images and video, *IEEE Trans. Pattern Anal. Mach. Intell.* 2 (3) (2001) 800–810. (8).
- [18] Wangenheim, et al., Color image segmentation using an enhanced Gradient network method, *Pattern Recognition Lett.* 30 (2009) 1404–1412.
- [19] Q.Luo Khoshgoftaar, Unsupervised multiscale color image segmentation based on MDL principle, *IEEE Trans. Syst. Man. Cybern.* 15 (9) (2006) 100–104.
- [20] S.Ji, H.W.Park, Image segmentation of color image based on region coherency, *International Conference on Image Processing*, pp. 80–83, 1998.
- [21] Shamir Lior, Human Perception based color segmentation using fuzzy logic, *Int. Conf. Fuzzy Syst.* 2 (2006) 496–505.
- [22] Y.W. Lim, S.U. Lee, On the colour image segmentation algorithm based on thresholding and the fuzzy c-means techniques, *Pattern Recognition* 23 (3) (1990) 935–952.
- [23] H.D. Cheng, J. Li, Fuzzy homogeneity and scale space approach to color image segmentation, *ICCV* (2000).
- [24] C.H. Oh, K. Honda, H. Ichihashi, Fuzzy clustering for categorical and multivariate data, *Proc. IFSA/NAFIPS* 4 (2001) 2154–2159.
- [25] K. Kummamuru, A. Dhawale, R. Krishnapuram, Fuzzy co-clustering of documents and keywords, *IEEE Conf. Fuzzy Syst.* 2 (2003) 772–777.
- [26] W.C. Tjhi, L. Chen, Possibilistic fuzzy co-clustering of large document collections, *Pattern Recognition* 40 (2007) 3452–3466.
- [27] W.C. Tjhi, L. Chen, Robust fuzzy co-clustering algorithm, *IEEE Conf. ICICS* (2007).
- [28] Guan, Qiu, Yang Xue, Spectral images and features co-clustering with application to content based image retrieval, in: Proc. IEEE Workshop Multimedia and Signal Processing, October 2005, pp.1–4.
- [29] Qiu, Image and feature co-clustering, in: Proceedings of IEEE Conference on Pattern Recognition, 2004, pp.1051–1054.
- [30] M. Hanmandlu Seba Susan, V.K.Madasu, B.C.Lovell, Fuzzy co-clustering of medical images using bacterial foraging, *IEEE Conference on Image Vision and Computing*, New Zealand, November 2008.
- [31] G. Wyszecki, W.S. Stiles, *Color Science—Concepts and Methods, Quantitative Data and Formulae*, Wiley Inter-Sc. Publications, New York, 2000.
- [32] G.H.Gomez, et al., Natural image segmentation using the CIElab space, *International Conference on Electrical, Computer, Electronics and communications*, pp. 107–110, 2009.
- [33] X.L. Xie, G. Beni, A validity measure for fuzzy clustering, *IEEE Trans. Pattern Anal. Mach. Intell.* 13 (1991) 841–847.
- [34] K. Rose, Gurewitz, Fox, Statistical mechanics and phase transitions in clustering, *Phys. Rev. Lett.* 65 (8) (1990) 945–949.
- [35] E.T. Jaynes, Information theory and statistical mechanics, *Phys. Rev. Lett.* 106 (1957) 620–630.
- [36] Miyamoto, Mikaidono, Fuzzy c-means as a regularization and maximum entropy approach, 7th IFSA World Congress, 1997, pp. 86–92.
- [37] J.C. Bezdek, *Pattern Recognition With Fuzzy Objective Function Algorithms*, Plenum Press, New York, 1981.
- [38] M.I. Chacon, L. Aguilar, A. Delgado, Definition and applications of a fuzzy image processing scheme, *IEEE Workshop Signal Process.* (2002) 102–107.
- [39] K.M. Passino, Biomimicry of bacterial foraging, *IEEE Control Syst. Mag.* (2002) 52–67.
- [40] M. Hanmandlu, O.P. Verma, N. Krishna Kumar, M. Kulkarni, A novel optimal fuzzy system for color image enhancement using bacterial foraging, *IEEE Transactions on Measurements and Instrumentation*, vol. 58, no. 8, pp. 2867–2879.
- [41] J.Liu Yang, Multi resolution color image segmentation, *IEEE Trans. Pattern Anal. Mach. Intell.* 16 (7) (1994) 530–549.
- [42] W.M. Rand, Objective criteria for the evaluation of clustering methods, *J. Am. Stat. Assoc.* 66 (336) (1971) 846–850.
- [43] R. Unnikrishnan, M. Herbert, Measures of similarity, in: Proceedings of IEEE Workshop Computer Vision Application, 2005.
- [44] The Berkeley Segmentation Dataset and Benchmark. [Online] <http://www.eecs.berkeley.edu/Research/Projects/CS/vision/bbsd/>.
- [45] D. Martin, C. Fowlkes, D. Tal, J. Malik, A database of human segmented natural images and its application to evaluating segmentation algorithms and measuring ecological statistics, *Proc. Int. Conf. Comput. Vision* 2 (2001) 416–423.
- [46] Chenglong Tang, Shigang Wang, Wei Xu, New fuzzy c-means clustering model based on the data weighted approach, *Data Knowl. Eng.* 69 (9) (2010) 881–900.
- [47] Xiao Ho Bargeila, Automatic brain MRI segmentation scheme based on feature weighting factors selection on fuzzy c-means clustering algorithms with Gaussian smoothing, *Int. J. Comput. Intell. Bioinf. Syst. Biol.* 1 (3) (2010), February.
- [48] K.S. Chuang, H.L. Tzeng, S. Chen, J. Wu, T.-J. Chen, Fuzzy c-means clustering with spatial information for image segmentation, *Comput. Med. Imaging Graphics* 30 (2006) 915.
- [49] Yuru Shilong Wang, Xu, Yongjie Pang, A fast underwater optical image segmentation algorithm based on a histogram weighted fuzzy c-means improved by PSO, *J. Mar. Sci. Appl.* 10 (1) (2011) 70–75.
- [50] N. Pal, K. Pal, J. Bezdek, A possibilistic fuzzy c-means clustering algorithm, *IEEE Trans. Fuzzy Syst.* 13 (4) (2005) 517–530.
- [51] P. Schmid, Segmentation of digitized dermatoscopic images by two-dimensional color clustering, *IEEE Trans. Med. Imaging* 18 (2) (1999) 164–171.



Madasu Hanmandlu (M'02) received the B.E. degree in Electrical Engineering from Osmania University, Hyderabad, India, in 1973, the M.Tech. degree in power systems from R.E.C. Warangal, Jawaharlal Nehru Technological University (JNTU), India, in 1976, and the Ph.D. degree in control systems from Indian Institute of Technology, Delhi, India, in 1981. From 1980 to 1982, he was a Senior Scientific Officer in Applied Systems Research Program (ASRP) of the Department of Electrical Engineering, IIT Delhi. He joined the EE department as a lecturer in 1982 and became Assistant Professor in 1990, an Associate Professor in 1995 and finally a Professor in 1997. He was with Machine Vision Group, City University, London, from April–November, 1988, and Robotics Research Group, Oxford University, Oxford from March–June, 1993, as part of the Indo-UK research collaboration. He was a Visiting Professor with the Faculty of Engineering (FOE), Multimedia University, Malaysia from March 2001 to March 2003. He worked in the areas of Power Systems, Control, Robotics and Computer Vision, before shifting to fuzzy theory. His current research interests mainly include Fuzzy Modeling for Dynamic Systems and applications of Fuzzy logic to Image Processing, Document Processing, Medical Imaging, Multimodal Biometrics, Surveillance and Intelligent Control. He has authored a book on Computer Graphics in 2005 under PBP publications and also has well over 220 publications in both conferences and journals to his credit. He has guided 20 Ph.D.s and 120 M.Tech students. He has handled several sponsored projects. He was an Associate Editor of both Pattern Recognition Journal (January 2005–March 2011) and of IEEE Transactions on Fuzzy Systems and a reviewer to other journals such as Pattern Recognition Letters, IEEE Transactions on Image Processing and Systems, Man and Cybernetics (January 2007–January 2010). He is a senior member of IEEE and is listed in Reference Asia; Asia's who's who of Men and Women of achievement; 5000 Personalities of the World (1998), American Biographical Institute. He was a Guest Editor of Defense Science Journal for the special issue on "Information sets and Information Processing" September, 2011



Om Prakash Verma received his B.E. degree in Electronics and communication Engineering from Malaviya National Institute of Technology, Jaipur, India, M. Tech-degree in Communication and Radar Engineering from Indian Institute of Technology (IIT), Delhi, India and Ph.D. in the area of soft and evolutionary computing and image processing from University of Delhi, Delhi, India. From 1992 to 1998 he was assistant professor in Department of ECE at Malaviya National Institute of Technology, Jaipur, India. He joined Department of Electronics and Communication Engineering, Delhi Technological University (formerly Delhi College of Engineering) as Associate Professor in 1998. Currently, he is Professor and Head, Department of Information Technology Delhi Technological University, Delhi India. He is also the author of more than 30 publications in

both International Conference Proceeding and Journal. He has guided more than 30 M. Tech student for their thesis and presently 5 Ph.D. research scholars are working under his supervision. He has authored a book on Digital Signal Processing in 2003. His present research interest includes: Applied soft computing, Artificial intelligent, Evolutionary computing, Image Processing, Digital signal processing. He is also a Principal investigator of an Information Security Education Awareness project, sponsored by Department of Information Technology, Government of India.



Seba Susan is currently a student of doctoral studies in Electrical Engineering Department in the Indian Institute of Technology, Delhi. Her areas of interest include Image processing, Pattern Recognition, Fuzzy-Neural Networks.



V.K. Madasu obtained Bachelor of Technology degree in Electronics and Communication Engineering with distinction from Jawaharlal Nehru Technological University, India in 2002 and Ph.D. in Electrical Engineering from the University of Queensland, Australia in 2006. From 2006–2008, he was a Research Associate in the School of Engineering Systems at Queensland University of Technology where he developed innovative Image Processing and Fuzzy Logic based technologies for diverse industrial applications. Currently, he is a Senior Research Officer at Tetra Q, University of Queensland, Australia working in the field of Medical Image Analysis. Vamsi is a member of IEEE, Computer Society and is listed in Who's Who in the World.